Experimental study of bubble resonant oscillations using a two-frequency acoustic technique

K. Ohsaka and E. H. Trinh

Jet Propulsion Laboratory, California Institute of Technology, Pasadena, California 91109

(Received

Abstract

A two-frequency acoustic apparatus has been developed to study the dynamics of a single gas or vapor bubble in water. An advantage of the apparatus is its capability of trapping a bubble by an ultrasonic standing wave while independently driving it into oscillations using a second lower frequency acoustic wave. As a preliminary application, the apparatus is used to study resonant oscillations. First, near-resonant coupling between the volume and the n = 3 shape oscillation modes of air bubbles at room temperature is studied, where n is the mode number. The stability boundary, amplitude vs. frequency, of the volume oscillation forms a wedge centered at the resonant frequency, which qualitatively agrees with a theoretical prediction based on a phase-space analysis. Next, the resonant volume oscillations of vapor bubbles are studied. The resonant radius of vapor bubbles at 80 °C driven at 1682 Hz is determined to be 0.7 mm, in agreement with a prediction obtained by numerical simulation.

resonant coupling
ultrasonic levitator

PACS numbers: 43.25.Yw, 43.25.Uv, 43.25.Zx

INTRODUCTION

Single bubble dynamics has been experimentally studied using acoustic techniques for several decades. The techniques involve trapping a bubble in a fluid host and driving the into either a volume (radial) or shape oscillation mode. Trapping can be accomplished by creating an ultrasonic standing wave in the fluid. A bubble can be trapped at a pressure antinode if its equilibrium radius, R_0, is smaller than the resonant radius, R_{res}, or at a node if R_0 is larger than R_{res}. For the bubble trapped at an antinode, the time-varying ultrasonic pressure field can be used to directly drive the bubble into oscillations[1,2]. However, this technique does not allow the variation of the driving frequency, and is only practical for small bubbles (typically $R_0 < 100$ μm) because of the weakening trapping capability at longer wave lengths. For the bubble trapped at a pressure node, modulation of the ultrasonic standing wave can be used to drive the bubble into oscillations[3,4]. This technique allows the variation of the driving frequency, but it uses the modulated acoustic radiation pressure to deform the trapped bubble. As a consequence, the volume oscillations can only be driven through nonlinear coupling between the shape and volume oscillations. It should also be noted that the trapped bubble may be driven using different time-varying fields such as an electrostatic field for certain fluids. In the light of these limitations associated with existing methods, we have developed an apparatus which employs two separate acoustic waves to independently trap and drive a bubble into volume and shape oscillations.

Volume and/or shape oscillations of gas or vapor bubbles play a major role in phenomena occurring in nature and in industrial processes. For example, part of ocean ambient noise is originated from oscillating bubbles created by natural processes. It is known that the efficiency of mass and heat transports in industrial processes is enhanced by oscillating bubbles in fluids. An improved understanding of the fundamentals of bubble

oscillations should contribute to better predictions of natural phenomena and more precise control of industrial processes. An objective of this study is to apply the present apparatus to verify some theoretically predicted features of oscillating bubbles. First, we consider the coupling between the volume and shape modes, which occurs because the bubble dynamics are intrinsically nonlinear. So far, this subject has mainly been studied theoretically[5-7]. Some of the predictions can be verified experimentally such as the existence of the one-two resonant coupling and the amplitude threshold for near-resonant coupling. Next, the vapor bubble resonance, which has unique features due to the interaction between dynamic and thermal processes[8-11]. It has been predicted that a vapor bubble has two resonant radii at the same frequency, and that these radii are significantly smaller than the resonant radius of gas bubbles at the same frequency.

I. EXPERIMENT

A. Apparatus

Figure 1 schematically shows the apparatus. The cell is a hollow cylindrical quartz tube whose outer diameter, wall thickness, and length are 15, 1, and 73 mm, respectively. The cell is approximately half filled with water in which a bubble is trapped. The bottom of the cell is directly cemented to the hollow cylindrical transducer. This transducer is driven at around 104 kHz to create an ultrasonic standing wave for trapping a bubble. The broadband audio speaker placed above the cell is operable up to 10 kHz, and can generate sound pressure which is sufficient to drive the trapped bubble into either the volume or shape oscillation mode. The nichrome heaters wound around the cell are used to raise the water temperature which is measured by a thermocouple. A single gas bubble is introduced in the water with a hypodermic syringe, and is trapped at a location between the two heaters, where the vertical temperature gradient is minimal at elevated temperatures.

The trapped bubble is back illuminated by the strobe light and its motion is monitored by the camera with a telescopic lens. The images of the bubble are recorded on videotape for later analysis.

B. Acoustic pressure estimation

The driving pressure generated by the audio speaker was estimated at room temperature using a dummy cell whose dimensions were exactly same as those of the actual cell. The dummy cell was placed under the audio speaker at exactly the same position as the actual cell and a calibrated hydrophone was inserted into the water from the bottom of the cell. There were two reasons to take this indirect method to estimate the pressure. First, the hydrophone could not be inserted into the water when a bubble was trapped because its presence disturbed the stability of the trapped bubble. Secondly, the magnitude of the driving audio frequency pressure was significantly lower than that of the ultrasonic pressure for bubble trapping, thus making the measurement of the audio frequency pressure variations difficult, if not impossible. The driving pressure generated by the audio speaker was correlated to the preamplified signal (input voltage) which was fed to the speaker through an amplifier.

Figure 2 shows an example of the driving pressure as a function of the input voltage at three driving frequencies. This example shows that the pressure is a function of both the input voltage and the driving frequency. It was noticed that the magnitude of the pressure is sensitive to the position of the water surface; therefore, the measurement was repeated at different surface positions near the surface position in the actual cell. It is found that the pressure always linearly increases as the voltage increases independent from the surface position. The offset from the origin seen in the figure is due to a minimum input voltage which is required to drive the audio speaker.

Figure 3 shows the driving pressure as a function of the driving frequency when the input voltage is maintained at 0.1 V. The pressure is widely scattered but it is clear that the cell shows a resonant condition at around 2000 Hz. The solid line is the average of the nine measurements. To estimate the pressure in the actual cell at different input voltages, the average value at 0.1 V at a corresponding frequency in Figure 3 was selected and linearly interpolated (extrapolated) to the different input voltages.

C. Observation procedure

1. Mode coupling

Outgassed distilled water was first introduced into the cell to a level about halfway to the top, then the ultrasonic transducer was turned on. The frequency was selected at around 104 kHz and then the water height was adjusted to generate a standing wave in the water. An air bubble was introduced in the water using a hypodermic syringe with a thin-gauge needle. The mode of the standing wave was not precisely known but bubbles could easily be trapped at several locations. We chose one near the axial center of the cell halfway to the surface. Once the bubble was stabilized, the audio speaker was turned on to drive the bubble. When the input voltage was low, the bubble was always driven in the volume mode. The speaker was tuned to the frequency, f_0, which approximately satisfies $f_0 = 2 f_n$, where f_n was the resonant frequency of the shape oscillation with the mode n. Then, the input voltage was gradually increased until the volume mode turned into a shape mode to determine the upper threshold value. Next, the input voltage was gradually reduced until the shape mode turned back to the volume mode to determine the lower threshold. The apparatus could generate a variety of the shape oscillation modes by varying the driving frequency. Some of them were simple and could be assigned to low order resonant modes. However, the majority displayed complicated and periodically changing shapes.

We decided to study coupling between the volume and the axisymmetric n = 3 shape oscillations.

2. Vapor bubble resonance

Outgassed distilled water was first introduced into the cell to a level about halfway to the top. The heater whose temperature was measured by an immersed thermocouple was then turned on. Once the temperature was stabilized, the ultrasonic transducer was turned on and the water height was adjusted to generate a standing wave in the water. Then, the thermocouple was withdrawn from the water because its presence disturbed the stability of the trapped bubble. A bubble was introduced in the water with a hypodermic syringe. The content of the bubble was initially air but it quickly became a mixture of air and saturated water vapor (roughly, 50/50 at 80 °C). The audio speaker was then turned on to drive the bubble in the volume oscillation. For this study, the driving frequency was set at 1682 Hz. Once the bubble was stabilized, the input voltage was gradually increased to a predetermined value, 0.1 V or just below the threshold value when the volume mode turned into the shape mode at the input voltage below 0.1 V. The images of the bubbles in the volume mode were recorded on videotape to determine the amplitude in later analysis. The same procedure was repeated for bubbles with different radii.

D. Image analysis procedure

The images of the oscillating bubbles were taken under strobe illumination to reveal the volume variation in a slow motion. The videotapes were reviewed and the images of bubbles were captured at a certain time interval and transferred into a computer using a commercially available software program. The 2-D image of the bubble was distorted into an oblate shape by the curvature of the cell wall in addition to the actual deformation due to

the acoustic pressure. Because the actual deformation was minimal and the vertical length was not optically distorted, we determined the actual radius of the bubble from the vertical bubble length and the known magnification of the image. The sequential images allowed us to determine the maximum and minimum radii from which we determined the amplitude of the volume oscillation. The possible errors due to the finite number of pixels of the camera were considered when the radius was determined.

II. RESULTS

Figure 4 shows sequential images of oscillating gas bubble, R_0 = 0.6 mm in the axisymmetic n = 3 mode at 1083 Hz. The spot near the center of the images is the highlight created by the back illuminating light. The sequence represents one cycle of the shape oscillation. Figure 5 shows the amplitude variations of the same bubble oscillating in the volume mode at slightly below the threshold and in the shape mode at slightly above the threshold. The relative amplitude of the volume mode is defined as the actual amplitude divided by R_0. For the shape mode, the relative amplitude is given by the vertical length between the top edge and the center of the image divided by R_0. The figure reveals a significant magnitude difference between the two modes at a similar driving pressure, and the resonant coupling condition, $f_0 \approx 2f_3$, being satisfied. It should be noted that the figure does not reveal the true phase relationship between the volume and the shape modes. A hysteresis effect is observed in the transition. As a consequence, the upper and lower thresholds are slightly different and they are determined to be 0.078 V and 0.070 V, respectively, in terms of the input voltage for this particular bubble. The experimental threshold pressure is estimated to be roughly 3 x 10^2 Pa using the value in Figure 3.

Figure 6 shows the stability boundary, amplitude vs. frequency, of gas bubble, R_0 = 0.44 mm, which is driven into the n = 3 shape oscillation with the one-two resonant

coupling condition. The open circles represent the measured threshold values. The straight lines are drawn to construct the boundary. The threshold amplitude at the resonant frequency is approximately 1.2 %.

To establish the correlation between the input voltage and the relative amplitude, the amplitude was measured at several input voltages. Figure 7 shows the correlation for three different bubbles driven at 1682 Hz at room temperature. As it is seen, the relative amplitude linearly increases as the input voltage increases. The offset from the origin is negligible. Although, for these three bubbles, the linear coefficient happens to be roughly the same, it should be different depending on the bubble radius, but the linear correlation is expected to be valid at small amplitudes for any size of bubbles.

Figure 8 summarizes the results of the amplitude measurement for both vapor and air bubbles driven at 1682 Hz. The figure shows the relative amplitude as a function of the bubble radius when the input voltage is maintained at 0.1 V. The open circles represent the vapor bubbles at 80 °C. The solid circles represent the air bubbles at room temperature. It should be noted that for some vapor bubbles, the volume mode could not be maintained at 0.1 V because it turned into the shape mode. In that case, the amplitude was determined at a reduced input voltage. Then, the amplitude was extrapolated to that of 0.1 V assuming the linear correlation. This correction is reflected in the large error bars of some data. Relatively large scattering of the vapor bubble data is partially due to the spatial instability caused by fluid convection around the bubble. As it is seen, the amplitude of the air bubbles is relatively constant throughout the measured size range. On the other hand, the amplitude of the vapor bubble shows the peak centered at 0.7 mm, which can be attributed to resonance.

III. DISCUSSION AND SUMMARY

We have developed a two-frequency acoustic apparatus which traps a bubble in a liquid host with a fixed frequency ultrasonic standing wave, and drives the bubble into oscillations with a variable low frequency sound wave. The apparatus is used to verify some theoretically predicted features associated with the resonant oscillations of gas and vapor bubbles. The apparatus, or more precisely the diagnostic technique will undergo improvements to reduce experimental uncertainties. The dummy cell technique produced a wide range scattering of the acoustic pressures. This wide range scattering is partially due to a resonance of the cell, which is not always reproducible. For this reason, we presented the acoustic pressure values simply as an estimate of order of magnitude in this paper. An improvement of the technique is necessary for a reliable estimation. Current imaging technique employs a standard video camera which has limited spatial and temporal resolutions. The implementation of a high speed camera or a laser scattering method for sizing the bubbles will allow us to perform better quantitative analysis.

We studied the so-called one-two near resonant coupling between the volume and the n = 3 shape oscillations of the air bubbles. Feng and Leal[7] theoretically studied the one-two resonant coupling using a phase-space analysis technique. They showed that the stability boundary of the volume oscillation formed a wedge centered at the frequency twice of the resonant frequency. The present result shows that the stability boundary forms a similar wedge, in agreement with their prediction. However, we did not observe the total instability of the volume mode at the resonant frequency as they predicted. There are several possible reasons for this discrepancy, but it is most likely due to the fact that the theory does not include appropriate damping of the oscillations. In the experimental side, one should note that the bubble is trapped by the ultrasound pressure at a much higher pressure level. On some occasions, high frequency capillary waves were visible on the

bubble surface even when the low frequency driving pressure was not present. Although these surface disturbances generally tend to induce shape oscillations, it is not clear how the capillary waves interact with the volume oscillation in the present experiment. Ultimately, this question can be answered if the experiment is performed under negligible ultrasonic pressure, which can be realized in a microgravity environment.

We drove vapor bubbles into volume oscillation to study resonance. The result clearly shows a peak in the amplitude, which suggests a resonant response. In order to exclude the possibility that the peak was caused by the apparatus characteristics, we also measured the oscillation amplitude of air bubbles under the same conditions except that the water was at room temperature. As seen, the air bubbles do not show the peak. Hao and Prosperetti[11] carried out a numerical study of vapor bubble resonance to examine the predictions of earlier analytical studies, such as the existence of two resonant radii. A relevant result of their study for comparison with the present result is the larger resonant radius of vapor bubble at 80 °C. They predict that the resonant radius of vapor bubble at 80 °C is 0.7 mm when the bubble is driven at around 1680 Hz. This prediction agrees with the present result which shows that the amplitude of the volume oscillation has the peak centered at 0.7 mm when the vapor bubbles are driven at 1682 Hz. The resonance is relatively weak (small peak height), which is probably due to the significant presence of the noncondensable gas (air) in the vapor bubbles. The reason why some of the vapor bubbles whose radii are close to 0.7 mm do not resonate is not known, but we suspect the presence of the ultrasonic pressure field which is much stronger than the driving pressure field. The dynamic response of the vapor bubble near the smaller resonant radius (< 0.1 mm) could not be tested because the minimum radius of bubbles which could be studied with the present apparatus was approximately 0.2 mm. The numerical study also predicted a

continuous growth of the vapor bubble, which could not be verified because of the limited resolution of the images taken by the present camera.

ACKNOWLEDGMENTS

We would like to thank Dan Barber for his help to construct the apparatus and Professor Prosperetti for providing his results prior to publication and his comments on early version of this manuscript. The research described in the paper was carried out at the Jet Propulsion Laboratory, California Institute of Technology, under contract with the National Aeronautics and Space Administration.

References

[1] R. G. Holt and L. A. Crum, "Acoustically forced oscillations of air bubbles in water: Experimental results," J. Acoust. Soc. Am. **91**, 1924-1932 (1992).

[2] D. F. Gaitan, L. A. Crum, C. C. Church and R. A. Roy, "Sonoluminescence and bubble dynamics for a single, stable, cavitation bubble," J. Acoust. Soc. Am. **91**, 3166-3183 (1992).

[3] T. J. Asaki, P. L. Marston and E. H. Trinh, "Shape oscillations of bubbles in water driven by modulated ultrasonic radiation pressure: observations and detection with scattered laser light," J. Acoust. Soc. Am. **93**, 706-713 (1993).

[4] E. H. Trinh, D. B. Thiessen and R. G. Holt, "Driven and freely decaying nonlinear shape oscillations of drops and bubbles immersed in a liquid: experimental results," J. Fluid Mech. **364**, 253-272 (1998).

[5] J. E. Ffowcs-Williams and Y. P. Cuo, "On resonant nonlinear bubble oscillations," J. Fluid Mech. **224**, 507-529 (1991).

[6] M. S. Longuet-Higgins, "Resonance in nonlinear bubble oscillations," J. Fluid Mech. **224**, 531-549 (1991).

[7] Z. C. Feng and L. G. Leal, "On energy transfer in resonant bubble oscillations," Phys. Fluids A**5**, 826-836 (1993).

[8] R. D. Finch and E. A. Neppiras, "Vapor bubble dynamics," J. Acoust. Soc. Am. **53**, 1402-1410 (1973).

[9] T. Wang, "Effects on evaporation and diffusion on an oscillating bubble," Phys. Fluids **17**, 1121-1121 (1974).

[10] P. L. Marston, "Evaporation-condensation resonance frequency of oscillating vapor bubbles," J. Acoust. Soc. Am. **66**, 1516-1521 (1979).

[11] Y. Hao and A. Prosperetti, "The dynamics of vapor bubble in acoustic fields," submitted to J. Fluid Mech.

Captions

Figure 1. Schematic diagram of experimental apparatus showing the key parts.

Figure 2. The driving low frequency pressure as a function of the input voltage at three driving frequencies, determined with the dummy cell.

Figure 3. The driving low frequency pressure as a function of the driving frequency when the input voltage is maintained at 0.1 V.

Figure 4. Sequential images of oscillating bubble in the n = 3 axisymmetric shape mode. The images are optically distorted due to the curvature of the cell. The spot near the center of the images is the highlight created by the illuminating light.

Figure 5. The amplitude variation of bubble (R_0 = 0.6 mm) oscillating in the volume and n = 3 shape modes, driven at 1083 Hz..

Figure 6. The stability boundary, amplitude vs. frequency, of the volume mode for the bubble (R_0 = 0.44 mm) driven into the n = 3 shape mode.

Figure 7. The correlation between the input voltage and the relative amplitude for three different bubbles, driven at 1682 Hz.

Figure 8. The relative amplitudes as a function of the bubble radius for air and vapor bubbles, driven at 1682 Hz when the input voltage is maintained at 0.1 V.

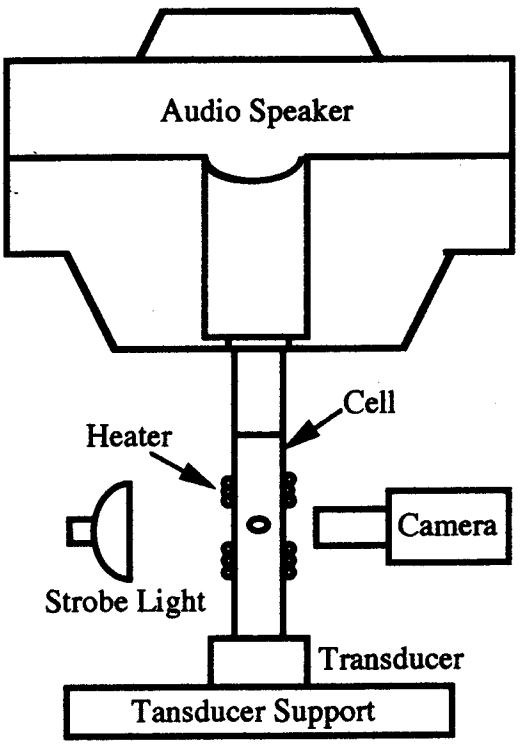

Fig. 1, K. Ohsaka, JASA

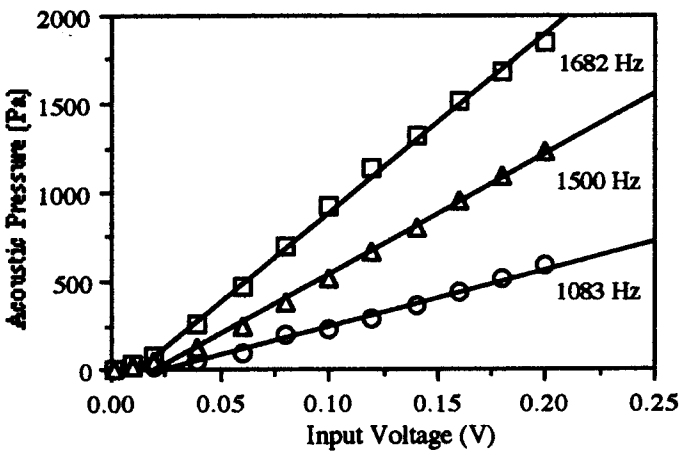

Fig. 2, K. Ohsaka, JASA

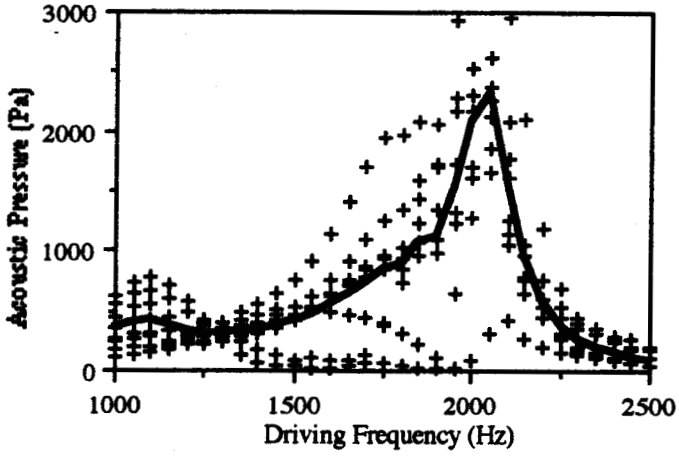

Fig. 3, K. Ohsaka, JASA

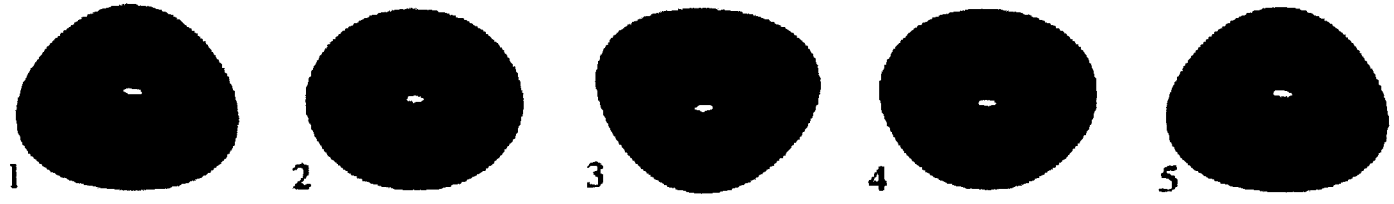

Fig 4. K. Chisaka, JASA

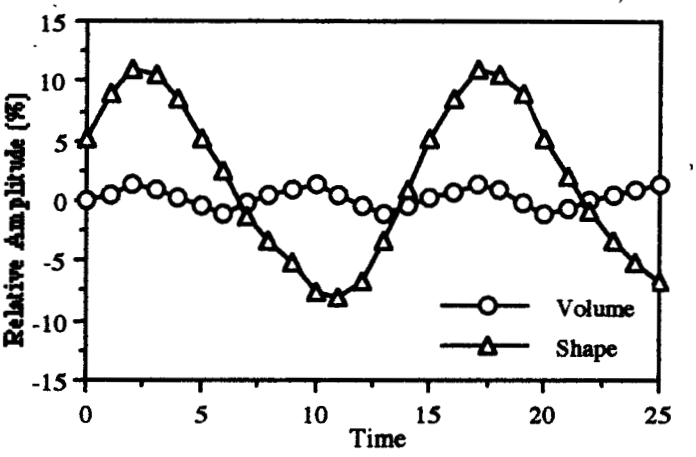

Fig. 5, K. Ohsaka, JASA

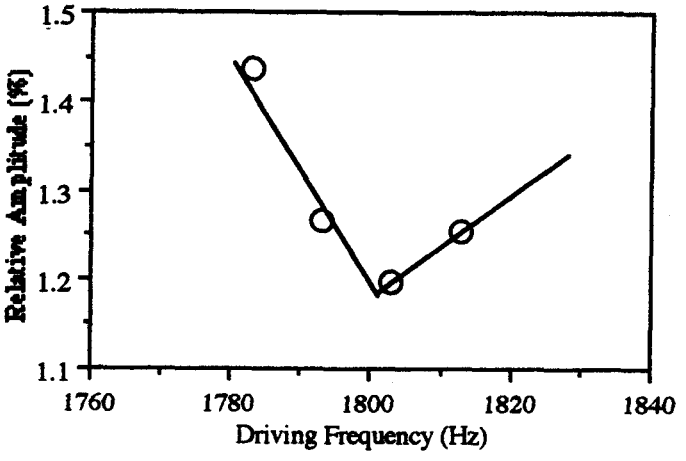

Fig. 6. K. Ohsaka, JASA

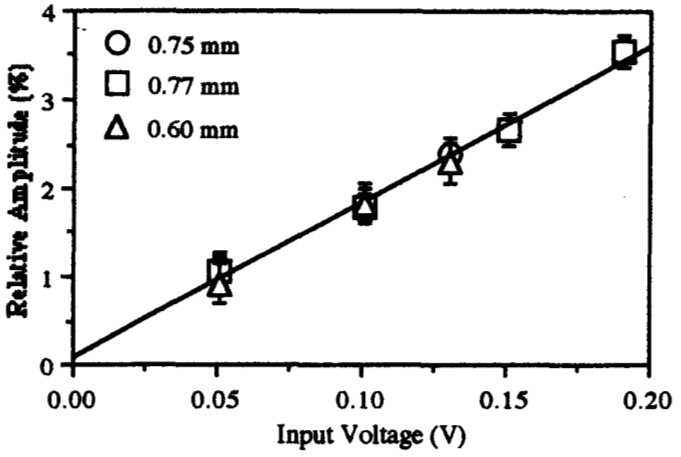

Fig. 7, K. Ohsaka, JASA

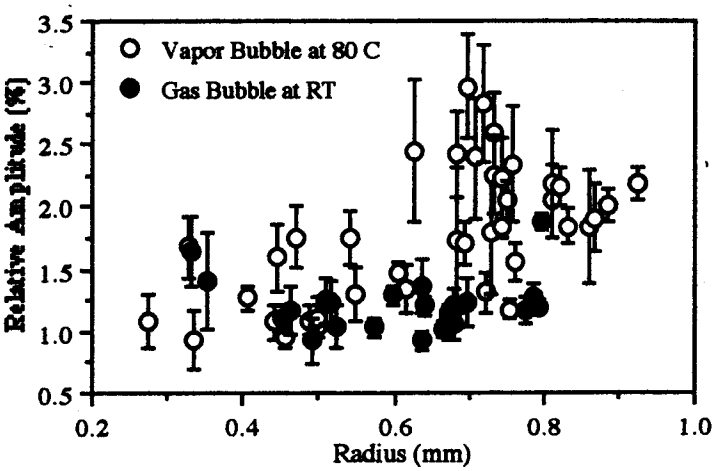

Fig. 8. K. Ohsaka, JASA